Available online at www.sciencedirect.com
ScienceDirect
Acta Materialia 56 (2008) 2649–2662
Acta MATERIALIA
www.elsevier.com/locate/actamat

Morphologies, orientation relationships and evolution of Cu_6Sn_5 grains formed between molten Sn and Cu single crystals

H.F. Zou, H.J. Yang, Z.F. Zhang *

Shenyang National Laboratory for Materials Science, Institute of Metal Research, Chinese Academy of Sciences, Shenyang 110016, China

Received 20 January 2008; received in revised form 30 January 2008; accepted 31 January 2008
Available online 14 March 2008

Abstract

The morphologies and orientation relationships of Cu_6Sn_5 grains formed between Sn and (0 0 1), (0 1 1), (1 1 1) and (1 2 3) Cu single crystals under liquid- and solid-state aging conditions were systematically investigated. The regular prism-type Cu_6Sn_5 grains formed on (0 0 1) and (1 1 1) Cu single crystals are elongated either along two perpendicular directions or along three preferential directions with an angle of 60° between each pair of directions. The orientation relationships between Cu and Cu_6Sn_5 lattice structures were determined by electron backscatter diffraction and were explained in terms of their minimum misfit. However, on (0 1 1) and (1 2 3) Cu single crystal surfaces, the Cu_6Sn_5 grains were mainly scallop-type, with only a few regular prism-type grains. Furthermore, the regular prism-type Cu_6Sn_5 grains will change into scallop-type after long reflow or aging times. Meanwhile it is considered that the growth of the scallop-type grains is supplied by two fluxes: the flux of the interfacial reaction and the flux of ripening. However, the growth of the prism-type grains is only supplied by the flux of the interfacial reaction. The kinetics of IMCs growth between Sn and Cu single crystals was also investigated.

Keywords: Cu single crystal; Orientation; Intermetallic compounds (IMCs); Coarsening mechanism; Growth kinetics

1. Introduction

Sn–Pb alloys have widely been used in industry for many years [1,2]. However, in the European Union, the use of Pb in electronics was prohibited from 1 January 2008 because Sn–Pb alloys cause serious pollution to environment [3]. Therefore, the interfacial reactions between lead-free solders (Sn–Ag, Sn–Ag–Cu and Sn–Cu) and substrates as well as their mechanical properties have attracted much attention from many researchers [1–10]. In these Sn-based alloys, Sn is the main element and reacts with the substrate to form Cu–Sn or Ni–Sn intermetallic compound (IMC) layers. In addition, polycrystalline Cu substrate is currently widely used in electronics, and forms Cu_6Sn_5 grains with scallop-type morphology – a finding that is well explained by the ripening reaction [11].

However, a recent study found that elongated and rooftop-type Cu_6Sn_5 grains formed on (0 0 1) Cu single crystal substrate [12]. The elongations align along two perpendicular directions. In particular, the rooftop-type Cu_6Sn_5 grains have a strongly preferred orientation. In addition, Prakash et al. observed that the Cu_6Sn_5 layer displayed a strong texture feature [13]. It is reasonable to suppose that the nucleation, growth and ripening behaviors of Cu_6Sn_5 on Cu single crystal substrate may be quite different from the conventional case of wetting on a polycrystalline Cu surface. In the current study, in order to avoid the effect of other elements, pure Sn was used as a solder, and four groups of Cu single crystals with wetting planes of (0 0 1), (1 1 1), (0 1 1) and (1 2 3) were specially designed as substrates. We employed these pure Sn/Cu couples as examples to reveal the effect of the crystallographic orientations of Cu single crystals on the morphologies,

* Corresponding author. Tel.: +86 24 23971043.
E-mail address: zhfzhang@imr.ac.cn (Z.F. Zhang).

1359-6454/$34.00 © 2008 Acta Materialia Inc. Published by Elsevier Ltd. All rights reserved.
doi:10.1016/j.actamat.2008.01.055

orientation relationships and evolution of Cu_6Sn_5 grains during liquid-state and solid-state interfacial reactions. Finally, the growth kinetics of Cu_6Sn_5 grains formed between pure Sn and Cu single crystal substrates with different orientations was discussed.

2. Experimental procedure

In this study, Cu single crystals were used as substrates and Sn foil was employed as solder. First, bulk Cu single crystal plate with dimensions of $40 \times 150 \times 10\ mm^3$ was grown from Cu bar with a purity of 99.999% by the Bridgman method in a horizontal furnace. The orientation of the Cu single crystal plate was determined by the electron backscattered diffraction (EBSD) method. Next, some pieces of Cu thin plates with dimensions of $10 \times 10 \times 1\ mm^3$ were spark-cut from the grown Cu single crystal plate, ensuring that the wetting surfaces are parallel to the (0 0 1), (0 1 1), (1 1 1), (1 2 3) planes, respectively. These Cu single crystal samples were ground successively with 800, 1000 and 2000 grade SiC paper and then carefully polished with 2.5, 1.5 and 0.5 μm polishing pastes. Wetting samples were prepared by reacting Sn foil (~70 μm thick) with these Cu single crystals at 260 °C for 5, 60, 320 and 600 s, respectively. These samples were then cooled in air to room temperature and ultrasonically cleaned in acetone for 10 min to remove the dissolved rosin mildly activated (RMA) on the Cu surface. Some samples wetted at 260 °C for 60 s were put into an oven at a constant temperature of 180 ± 2 °C and aged for 12, 36 and 180 h, respectively. After that, all the samples were deeply etched with the 5% HCl + 3% HNO_3 + CH_3OH (wt.%) etchant solution to remove the excess Sn phase so that the reactive phases can be fully exposed. In order to investigate the growth kinetics of the IMCs formed, the couples of Sn with (0 1 1), (1 1 1) and (1 2 3) Cu single crystal substrates were bonded in an oven with a constant temperature of 260 °C for 15 min and then these samples were isothermally aged at 170 ± 2 °C for 1, 3, 7, 12 and 18 days, respectively. Marker experiments were conducted in these couples. Each Cu single crystal was encircled with Mo wire before the bonding procedure, and the morphologies and thicknesses of the IMCs near the Mo wires were detected and measured each time. All the samples were observed with a LEO super35 scanning electron microscope (SEM) to detect the morphology of the IMCs.

3. Experimental results

3.1. Liquid-state reactions between Cu single crystals and molten Sn

Generally speaking, scallop-type Cu_6Sn_5 always forms on polycrystalline Cu surface after liquid-state reaction with SnAgCu at 260 °C for 60 s, as shown in Fig. 1; this has been widely observed previously [11,14,15]. For the Cu single crystal substrate, the IMC morphologies of the deep-etched Sn/(0 0 1) Cu soldering joints at 260 °C for different reflow times were investigated. Fig. 2a is a SEM image of Cu_6Sn_5 grains on the (0 0 1) Cu wetting plane at 260 °C for 5 s. It is obvious that the Cu_6Sn_5 grains display a regular prism-type rather than a scallop-type structure, and are distributed homogeneously across the whole (0 0 1) Cu surface, which is quite different from previous observations on Cu substrates [11,14–17]. This kind of Cu_6Sn_5 grain was named rooftop-type in Ref. [12]; hereafter, we will use the term prism-type to describe the morphology of the regular Cu_6Sn_5 grains. An interesting finding, from careful observations on these regular prism-type Cu_6Sn_5 grains, is that the elongations of Cu_6Sn_5 grains go along two perpendicular directions, which is consistent with Ref. [12], as indicated in Fig. 2a. Compared with the samples wetted at 260 °C for 5 s, the regularity of the prism-type Cu_6Sn_5 grains becomes much stronger when the reflow time increases to 60 s, as shown in Fig. 2b. The edge of the Cu_6Sn_5 grains becomes much sharper, and the size of the Cu_6Sn_5 grains increases slightly. Further increasing the reflow time up to 320 s results in no obvious change in the morphology of the Cu_6Sn_5 grains except for a small increase in the grain size, as shown in Fig. 2c. However, when the reflow time is increased to 600 s, the morphology of the Cu_6Sn_5 grains become quite different to that of the former samples. The regular prism-type Cu_6Sn_5 grains are almost entirely replaced by scallop-type grains on the entire (0 0 1) Cu surface. Only a few regular prism-type IMC grains appear at localized sites on the (0 0 1) Cu surface, as shown in Fig. 2d.

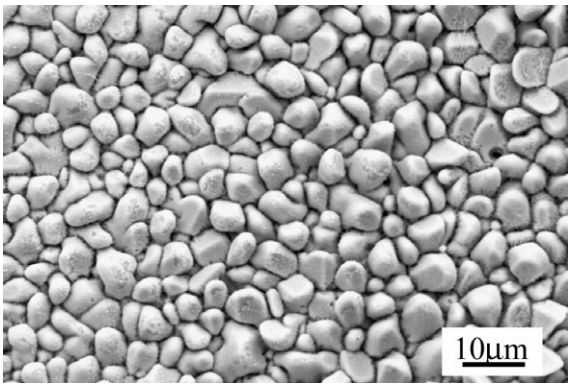

Fig. 1. Top view SEM image of scallop-type Cu_6Sn_5 grains on polycrystalline Cu.

Fig. 3 shows top-view SEM images of Cu_6Sn_5 grains formed on (0 1 1) Cu single crystal after reaction with Sn at 260 °C for different reflow times. It can clearly be seen that the morphology of Cu_6Sn_5 grains on (0 1 1) Cu single crystal is quite different from that on (0 0 1) Cu single crystal. The typical scallop-type Cu_6Sn_5 grains are homogeneously distributed across the whole (0 1 1) Cu surface when the samples were reflowed at 260 °C for 5 s, which is still consistent with the distribution on the polycrystalline Cu surface [11,14,15], as shown in Fig. 3a. When the reflow time increases to 60 s, some regular prism-type IMC grains

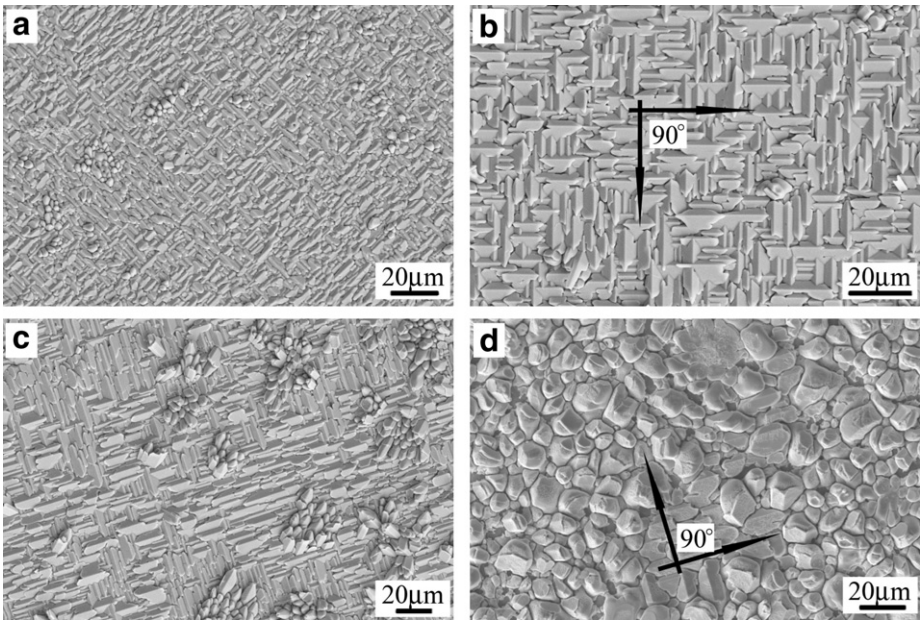

Fig. 2. Morphologies of prism-type Cu_6Sn_5 grains formed on (0 0 1) Cu single crystals at 260 °C for (a) 5 s, (b) 60 s, (c) 320 s, and (d) 600 s.

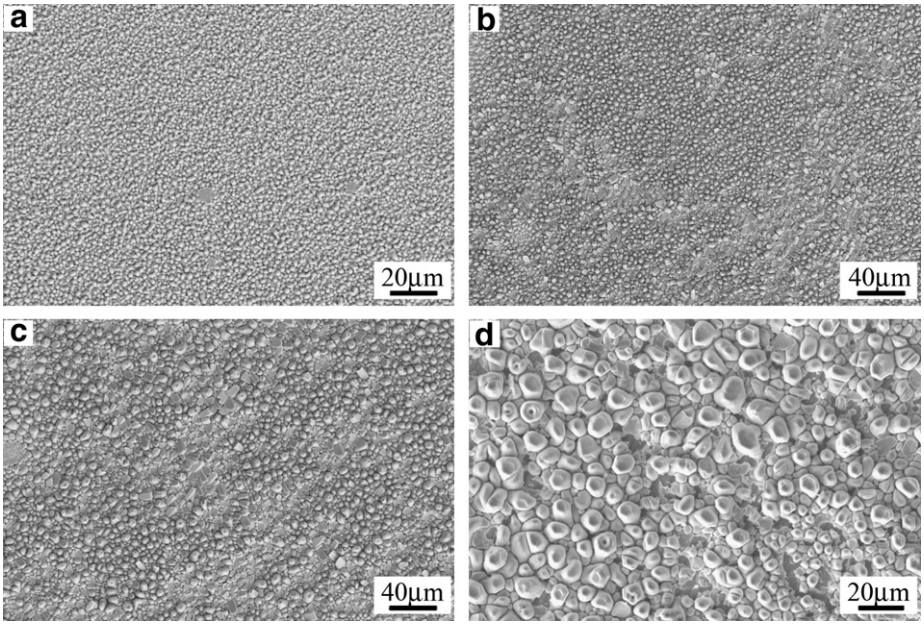

Fig. 3. Morphologies of prism-type Cu_6Sn_5 grains formed on (0 1 1) Cu single crystals at 260 °C for (a) 5 s, (b) 60 s, (c) 320 s, and (d) 600 s.

were observed on the (0 1 1) Cu single crystal surface, as indicated in Fig. 3b. For the sample reflowed for 320 s, the morphology of the Cu_6Sn_5 grains is the same as the grains reflowed for 60 s (Fig. 3c). Only scallop-like Cu_6Sn_5 grains are formed on the (0 1 1) Cu single crystal surface even when the reflow time increases up to 600 s, as shown in Fig. 3d.

Fig. 4 shows the morphologies of Cu_6Sn_5 grains formed on (1 1 1) Cu single crystal after reaction with Sn at 260 °C for different reflow times. It is interesting to see that the same regular prism-type Cu_6Sn_5 grains also appear on (1 1 1) Cu single crystal surfaces, as indicated in Figs. 2a and 4a. From careful observations on these regular prism-type Cu_6Sn_5 grains, one of the important findings is that the morphology of Cu_6Sn_5 grains on (0 0 1) Cu single crystal is different from that on (1 1 1) Cu single crystal. The prism-type Cu_6Sn_5 grains on (0 0 1) Cu single crystal align along two perpendicular directions, as shown in Fig. 2a. However, the prism-type Cu_6Sn_5 grains align along three different directions on (1 1 1) Cu single crystal, and their intersecting angles are approximately equal to 60°, as indicated in Fig. 4a. In order to investigate the morphology evolution of Cu_6Sn_5 grains formed between molten Sn and (1 1 1) Cu single crystal, several

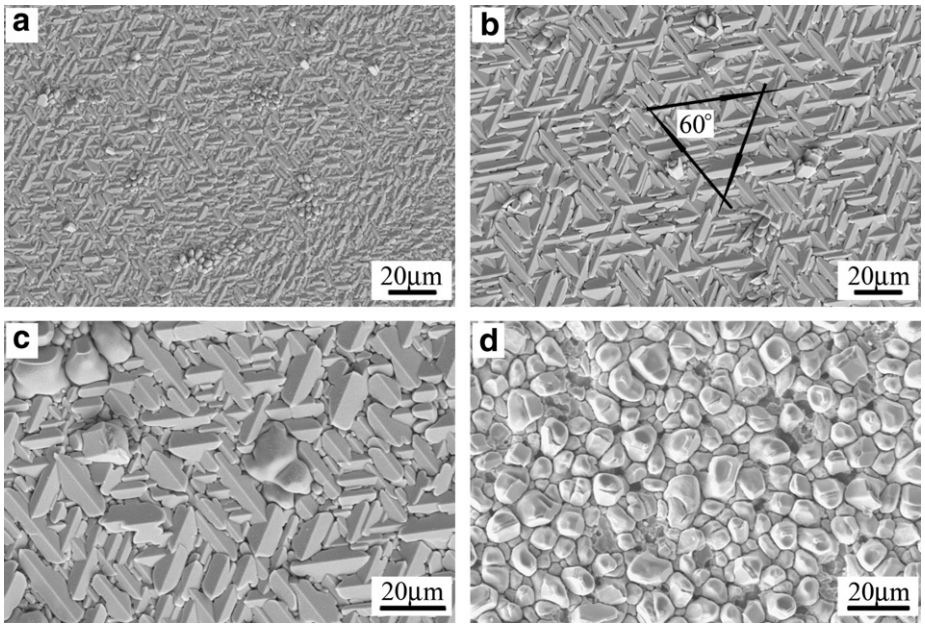

Fig. 4. Morphologies of prism-type Cu_6Sn_5 grains formed on (1 1 1) Cu single crystals at 260 °C for (a) 5 s, (b) 60 s, (c) 320 s, and (d) 600 s.

reflow times were tested in our experiment. Fig. 4b is an SEM image of Cu_6Sn_5 grains formed on the (1 1 1) Cu single crystal surface after reaction with Sn at 260 °C for 60 s. Compared with the image in Fig. 4a, the array of Cu_6Sn_5 grains is unchanged, but the edge of the Cu_6Sn_5 grains becomes rather sharp and the size of Cu_6Sn_5 grains increases somewhat, as displayed in Fig. 4b. When the reflow time further increases to 320 s, a few large scallop-type Cu_6Sn_5 grains were observed on the (1 1 1) Cu single crystal surface, and the prism-type Cu_6Sn_5 grains became much larger, as shown in Fig. 4c. However, prism-type Cu_6Sn_5 grains were not observed on the (1 1 1) Cu single crystal surface when the reflow time was increased to 600 s; almost all the Cu_6Sn_5 grains become scallop-type and were distributed across the whole (1 1 1) Cu single crystal surface (see Fig. 4d), as was found on the (0 0 1) Cu single crystal surface after prolonged aging.

Fig. 5 shows the morphologies of Cu_6Sn_5 grains formed on (1 2 3) Cu single crystal after reaction with Sn at 260 °C for different reflow times. For the sample wetted at 260 °C for 5 s, slantwise Cu_6Sn_5 cells were observed in a small region on the (1 2 3) Cu single crystal surface (Fig. 5a), which is different from the findings for the other three Cu

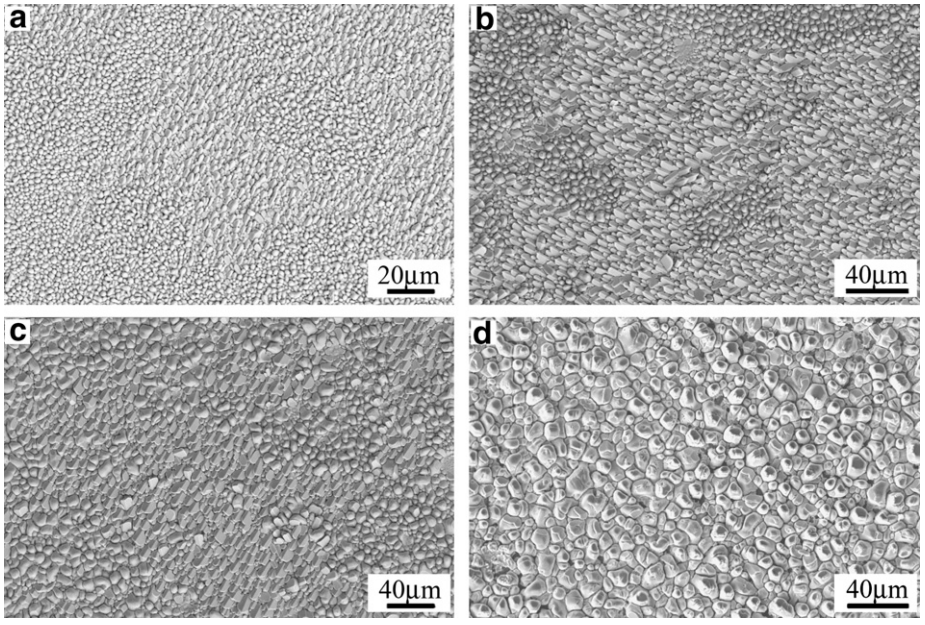

Fig. 5. Morphologies of prism-type Cu_6Sn_5 grains formed on (1 2 3) Cu single crystals at 260 °C for (a) 5 s, (b) 60 s, (c) 320 s, and (d) 600 s.

single crystal surfaces. Furthermore, the morphology of the Cu_6Sn_5 grains gradually becomes slantwise prism-type (like an array of knives) with increasing reflow time (60 s), as indicated in Fig. 5b. Further increasing the reflow time (320 s) results in no obvious change in the morphology of Cu_6Sn_5 grains except for an increase in the size of the grains, as shown in Fig. 5c. In contrast, for the sample wetted at 260 °C for 600 s, scallop-type Cu_6Sn_5 grains, rather than slantwise prism-type grains, were still detected on the (1 2 3) Cu single crystal surface.

3.2. Solid-state reactions between Cu single crystals and Sn

Fig. 6a is an SEM image of Cu_6Sn_5 grains formed on (0 0 1) Cu single crystal wetted with pure Sn at 260 °C for 60 s. Fig. 6b–d is the morphologies of the Cu_6Sn_5 grains on the (0 0 1) Cu single crystal surface after aging at 180 °C for different times. It can be seen that different morphologies of Cu_6Sn_5 grains form after different aging time. For short aging time (12 h), the regular aculeate prism-type Cu_6Sn_5 grains became larger and planar, and these regular Cu_6Sn_5 grains were surrounded by many scallop-type Cu_6Sn_5 grains, as shown in Fig. 6b. For the sample aged at 180 °C for 36 h, only a few prism-type Cu_6Sn_5 grains can be observed on the (0 0 1) Cu single crystal surface; instead, scallop-type Cu_6Sn_5 grains are distributed across almost the entire Cu surface (Fig. 6c). When the aging time is increased further to 180 h, scallop-type Cu_6Sn_5 grains instead of prism-type ones covered the entire (0 0 1) Cu single crystal surface, as shown in Fig. 6d.

Fig. 7 shows the morphologies of Cu_6Sn_5 grains formed on (0 1 1) Cu single crystal. It has been found that the regular prism-type Cu_6Sn_5 grains did not form on (0 1 1) Cu single crystal during the reflow procedure (see Fig. 7a). If the aging time at 180 °C is increased further, the morphology of Cu_6Sn_5 grains is unchanged though the size of the grains increases slightly (Fig. 7b–d). This is consistent with the interfacial reaction between Pb-free solder and polycrystalline Cu [11,14,15], and indicates that increasing aging time cannot induce the formation of the regular Cu_6Sn_5 grains on the (0 1 1) single crystal surface.

The effect of aging time on the morphology of Cu_6Sn_5 grains formed on (1 1 1) Cu single crystal was also investigated in our experiment. Fig. 8a is an SEM image of Cu_6Sn_5 grains formed on (1 1 1) Cu single crystal reflowed at 260 °C for 60 s. When the sample was aged at 180 °C for 12 h, the elongations of Cu_6Sn_5 grains also went along three directions, but the single prism-type Cu_6Sn_5 grain was not the same as that formed during the reflow procedure; the aculeate Cu_6Sn_5 grains were transformed into flat ones, as shown in Fig. 8b. The region containing the regular Cu_6Sn_5 grains became rather flat and a large number of scallop-type Cu_6Sn_5 grains were formed when the aging time further increased to 36 h (see Fig. 8c). When the aging time was further increased to 180 h, the scallop-type Cu_6Sn_5 grains completely replaced the prism-type ones and covered the entire (1 1 1) Cu single crystal surface, as shown in Fig. 8d. This demonstrates that the regular Cu_6Sn_5 grains formed on (1 1 1) Cu single crystal can also be transformed into irregular ones by increasing the aging time.

Fig. 9 illustrates the morphology evolution of Cu_6Sn_5 grains formed on (1 2 3) Cu single crystal. It can be seen that the regular prism-type Cu_6Sn_5 grains only appear at local regions on (1 2 3) Cu single crystal reflowed at 260° C for 60 s, as shown in Fig. 9a. When the samples were aged at 180 °C for more than 12 h, the scallop-type Cu_6Sn_5 grains are distributed across the whole (1 2 3) Cu single crystal surface. In particular, the Cu_6Sn_5 grains can

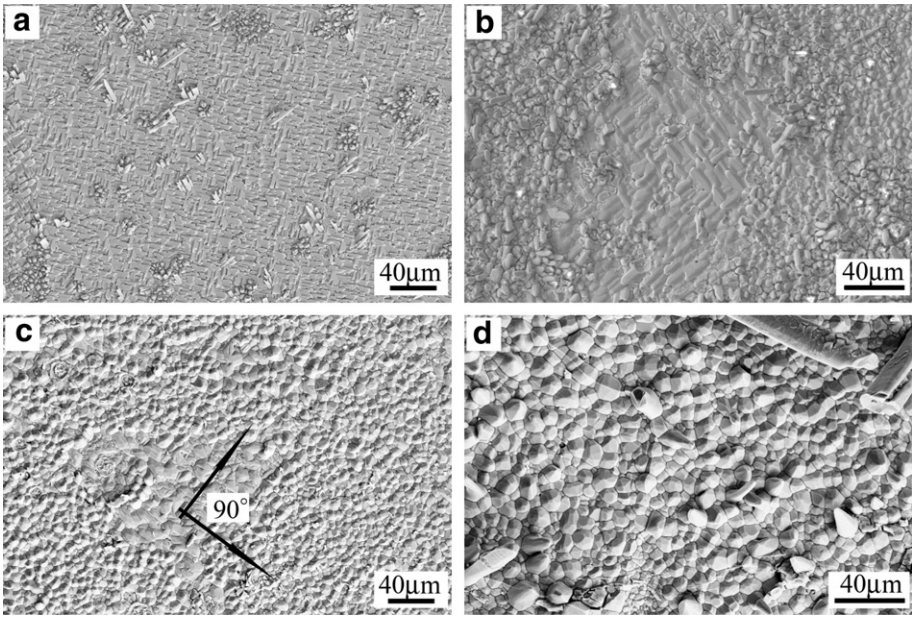

Fig. 6. Top view of the Cu_6Sn_5 grains formed on (0 0 1) Cu single crystal: (a) 60 s at 260 °C and at 180 °C for (b) 12 h, (c) 36 h, and (d) 180 h.

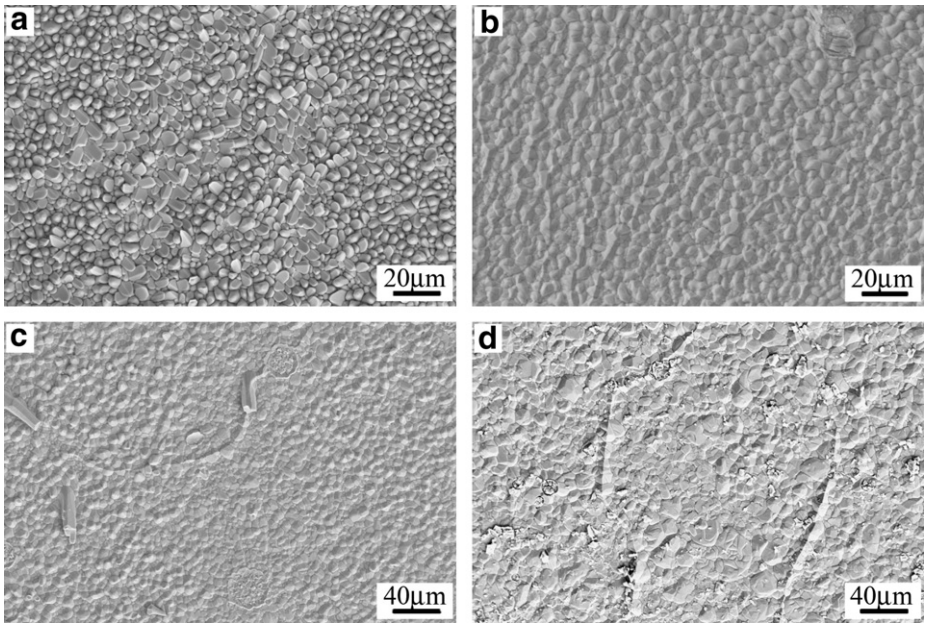

Fig. 7. Top view of the Cu_6Sn_5 grains formed on (0 1 1) Cu single crystal: (a) 60 s at 260 °C and at 180 °C for (b) 12 h, (c) 36 h, and (d) 180 h.

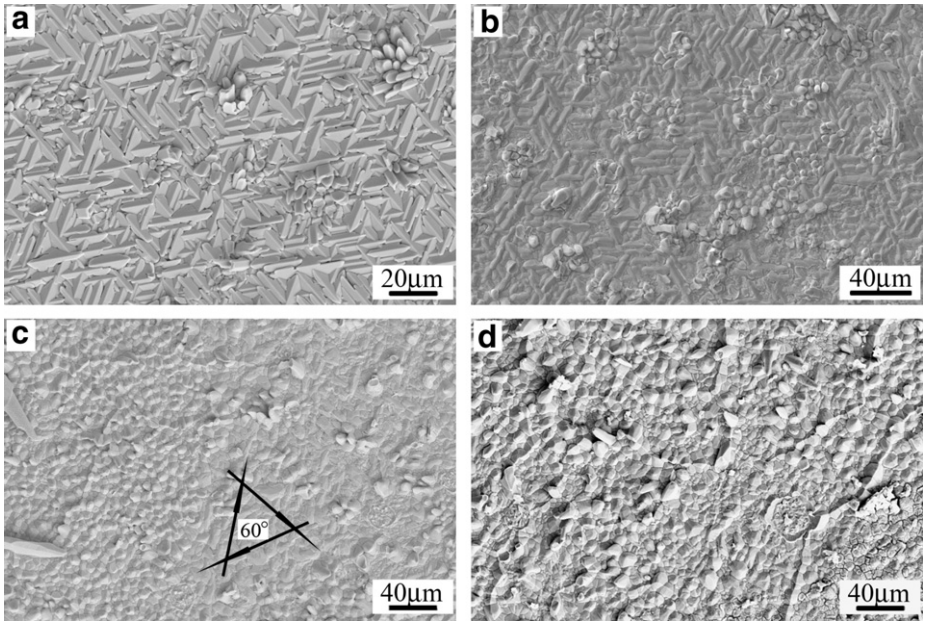

Fig. 8. Top view of the Cu_6Sn_5 grains formed on (1 1 1) Cu single crystal: (a) reflowing at 260 °C for 60 s and then aging at 180 °C for (b) 12 h, (c) 36 h, and (d) 180 h.

increase in size and flatten in morphology, as shown in Fig. 9b–d.

3.3. The growth kinetics of IMCs between Cu single crystals and Sn

Fig. 10 shows the morphologies of soldering joints between Sn and the Cu single crystals with different orientations after isothermal solid-state aging at 160 °C for different times. In order to observe the same interface each time, a Mo wire was used as a marker. Fig. 10a and b shows the two IMC layers (Cu_6Sn_5 and Cu_3Sn) of the joints between Sn and (0 1 1) Cu single crystal aged at 160 °C for 1 and 18 days, respectively, which is similar to most previous results [3,14,15]. As shown in Fig. 10c–f, similar results were observed for the other two couples: Sn/(1 1 1) Cu and Sn/(1 2 3) Cu.

Fig. 11 shows the dependence of the thickness of interfacial IMCs on the aging time for the couples between Sn and Cu single crystals with different orientations. It can be clearly seen that the thickness of the IMCs increases linearly with the square root of the aging time, which is

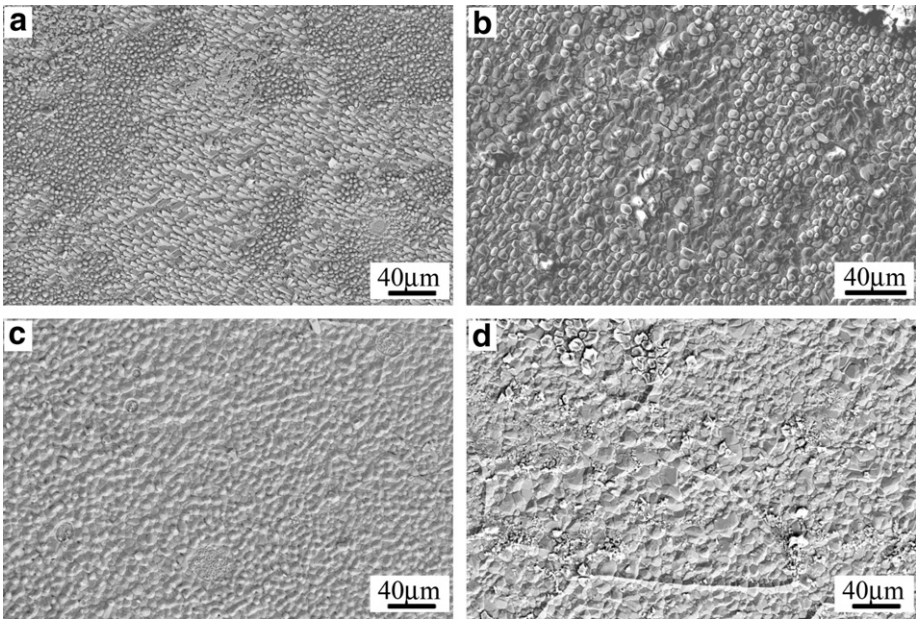

Fig. 9. Top view of the Cu_6Sn_5 grains formed on (1 2 3) Cu single crystal: (a) reflowing at 260 °C for 60 s and then aging at 180 °C for (b) 12 h, (c) 36 h, and (d) 180 h.

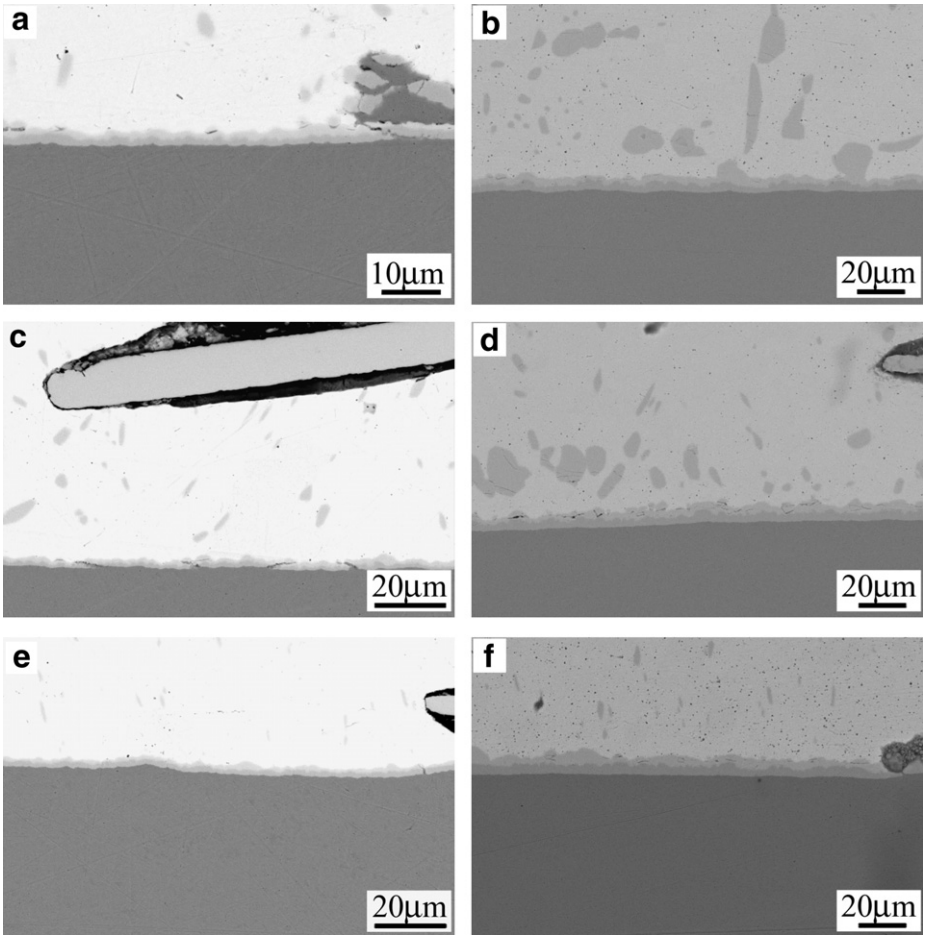

Fig. 10. SEM images taken at the Sn/Cu single crystal interface aging at 170 °C for different periods: (a) 1 day and (b) 18 days on (0 1 1) Cu single crystal substrate, (c) 1 day and (d) 18 days on (1 1 1) Cu single crystal substrate, (e) 1 day and (f) 18 days on (1 2 3) Cu single crystal substrate.

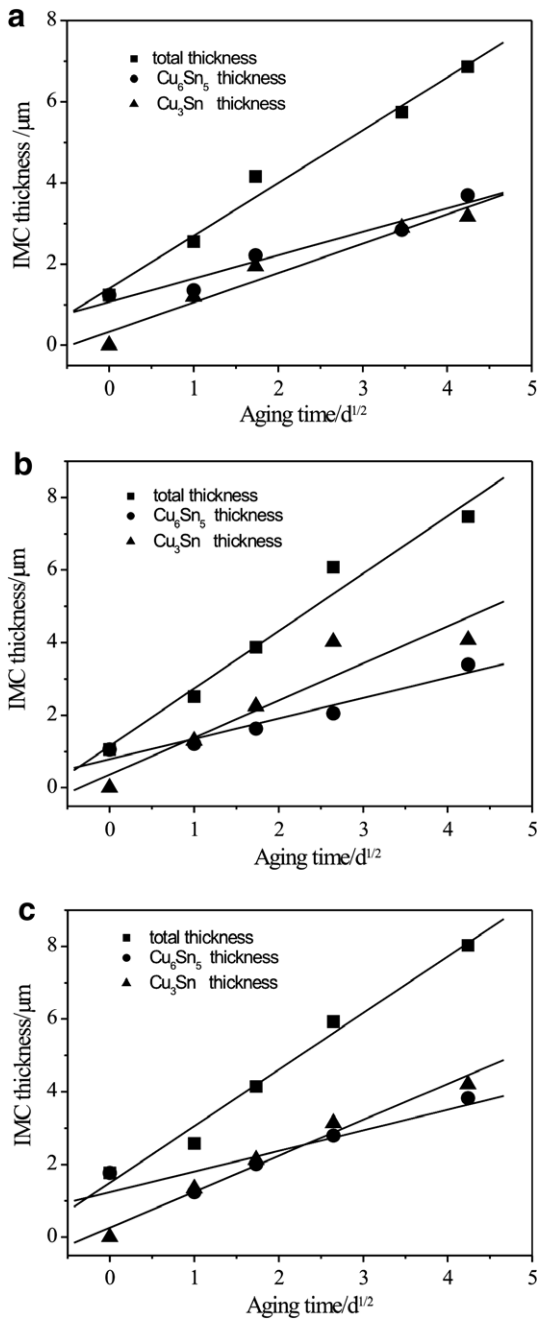

Fig. 11. Plot of the thickness of IMCs vs. different aging times at 170 °C: (a) on (011) Cu substrate, (b) on (111) Cu substrate, and (c) on (123) Cu substrate.

similar to the reaction between most solders and Cu substrate [18,19]. In addition, it is also noted that the growth velocity of Cu_3Sn layer is slightly faster than that of Cu_6Sn_5 layer on the three different Cu single crystal substrates, which is similar to the Sn–Ag–Cu/Cu single crystal [18]. Generally speaking, the growth kinetics of IMCs often follows the diffusion-controlled Fick's law [18]:

$$d = (Dt)^{1/2}, \quad (1)$$

where d represents the average thickness of IMCs, D is the diffusion coefficient, and t is the aging time. According to the data in Fig. 15, the values of D were calculated as 1.96×10^{-17}, 2.96×10^{-17} and $2.96 \times 10^{-17}\ m^2\ s^{-1}$ for (011), (111) and (123) Cu single crystals, respectively. The present results are smaller than the previous results for Sn–Ag–Cu/Cu single crystal, i.e. $7.24 \times 10^{-17}\ m^2\ s^{-1}$ at 170 °C [18] and Sn–Ag–Cu/polycrystalline Cu, i.e. $8.1 \times 10^{-17}\ m^2\ s^{-1}$ at 190 °C [19].

4. Discussion

4.1. Orientation relationships between Cu_6Sn_5 grains and Cu single crystals

As mentioned above, regular prism-type Cu_6Sn_5 grains were only observed on (001) and (111) Cu single crystal surfaces during the early wetting reaction procedure, as illustrated in Figs. 2 a–c and 4a–c. In addition, it is found that the morphologies of Cu_6Sn_5 grains on (001) Cu single crystal are also different from those on (111) Cu single crystal, as shown in Figs. 2b and 4b. According to these phenomena, there should be a preferential orientation relationship between the elongated Cu_6Sn_5 grains and the (001) and (111) Cu single crystals. It is assumed that the preferential orientations of Cu_6Sn_5 grains are not very obvious on the (123) Cu single crystal surface because only slantwise Cu_6Sn_5 grains were observed at localized regions, as shown in Fig. 5a–c.

Since each small prism-type Cu_6Sn_5 grain in Fig. 2 can be considered as a small Cu_6Sn_5 single crystal, it is possible to detect the orientation of each Cu_6Sn_5 grain by EBSD if the structure of the Cu_6Sn_5 grain can be obtained. Larsson et al. found that the η-Cu_6Sn_5 is stable only at high-temperatures (above 350 °C) and the η′-Cu_6Sn_5 is stable at temperatures below 350 °C [20,21]. In the current experiment, the wetting process was performed at 260 °C, so the η′-Cu_6Sn_5 phase with a monoclinic structure (C_2/c $a = 11.022$, $b = 7.282$, $c = 9.827$, $\beta = 98.84°$) was used in our EBSD analysis [20]. Therefore, the orientation of each Cu_6Sn_5 grain can be obtained from the Kikuchi bands.

Fig. 12 shows the Kikuchi bands of Cu single crystals and the Cu_6Sn_5 grains formed on them. In Fig. 12a and b, the Kikuchi bands were obtained from (001) and (111) Cu single crystals before the wetting experiment. Fig. 12c and d are the Kikuchi bands of two Cu_6Sn_5 grains elongated along two perpendicular directions formed on (001) Cu single crystal. The Kikuchi bands indicate that the crystallographic planes of the two Cu_6Sn_5 grains are the same along two perpendicular elongated directions. Further analysis illustrates that the (102) plane of Cu_6Sn_5 grain is parallel to the (001) plane of Cu. Fig. 12e–g are the Kikuchi bands of the three elongated Cu_6Sn_5 grains formed on (111) Cu single crystal, as indicated in Fig. 12h. The Kikuchi bands indicate that the crystallographic planes of the three Cu_6Sn_5 grains are also the same along the three elongated directions. Through careful analysis, the crystallographic planes of the Cu_6Sn_5 grains are approximately indexed as (010). Therefore, the (010) plane of Cu_6Sn_5 grain is parallel to the (111) plane of

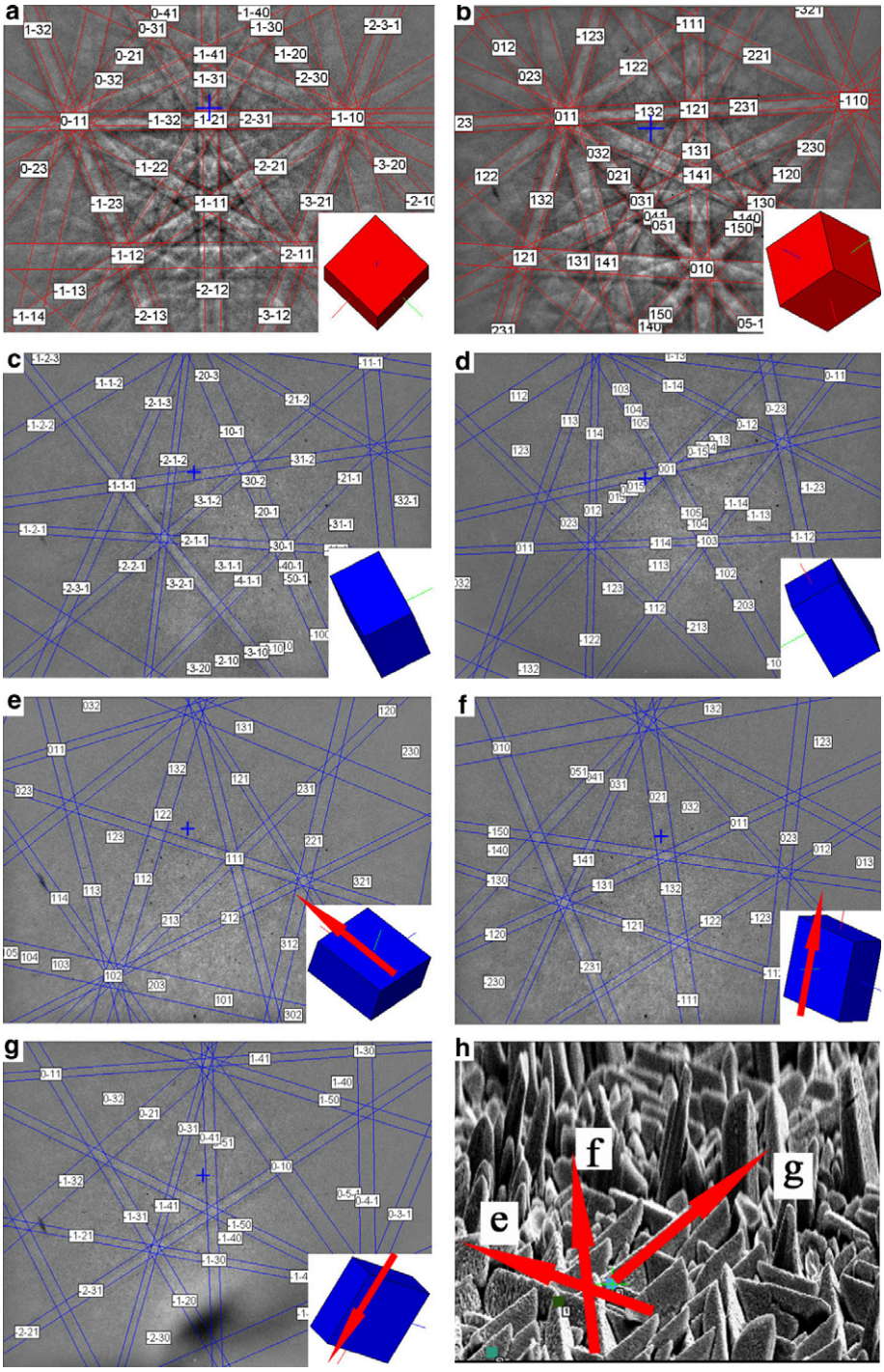

Fig. 12. (a, b) Kikuchi bands of (0 0 1) and (1 1 1) Cu single crystals; (c, d) Kikuchi bands of Cu_6Sn_5 grains along two perpendicular directions on (0 0 1) Cu single crystal; (e)–(g) Kikuchi bands of Cu_6Sn_5 grains along three different directions on (1 1 1) Cu single crystal; and (h) SEM image of Cu_6Sn_5 grains formed on (1 1 1) Cu single crystal along three different directions (corresponding to the Kikuchi bands in (e)–(g)).

Cu. The [1 0 0] direction of Cu_6Sn_5 grain in Fig. 12e–g is indicated by red arrows.[1] The angles between each elongated direction of Cu_6Sn_5 grains and the corresponding [1 0 0] direction of Cu_6Sn_5 grains were measured to be about 19.3°, 16.9° and 18.7°, respectively. After analyzing all the Kikuchi bands, four orientation relationships between Cu_6Sn_5 grains and (0 0 1), (1 1 1) Cu single crystals were obtained as follows:

$$(010)_{Cu_6Sn_5}||(001)_{Cu};\quad (102)_{Cu_6Sn_5}||(001)_{Cu},$$
$$(010)_{Cu_6Sn_5}||(111)_{Cu};\quad (102)_{Cu_6Sn_5}||(111)_{Cu}.$$

In our experiment, the strong texture of the Cu_6Sn_5 grains was only formed on (0 0 1) and (1 1 1) Cu single crys-

[1] For interpretation of color in Fig. 12, the reader is referred to the web version of this article.

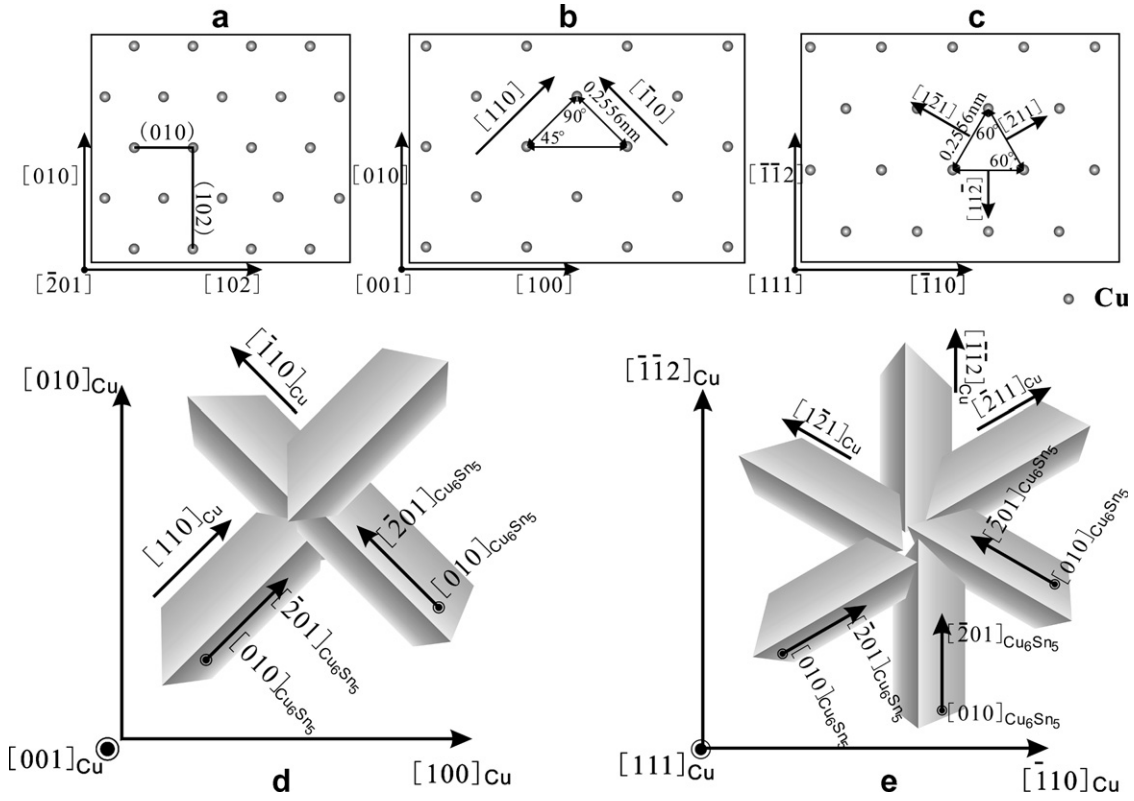

Fig. 13. (a) Structure of Cu_6Sn_5 cell projected from the [$\bar{2}$01] direction; (b) structure of Cu cell projected from the [001] direction; (c) structure of Cu cell projected from the [111] direction; and (d,e) schematic diagrams of the morphologies and orientations of Cu_6Sn_5 grains formed on (001) and (111) Cu single crystals.

tals instead of on polycrystalline Cu [11,14,15]. This shows that the regular array of atoms plays an important role in the formation of these strong textures in Cu_6Sn_5 grains. Fig. 13a shows the arrays of Cu atoms in Cu_6Sn_5 along the [$\bar{2}$01] direction. Fig. 13b and c shows the arrays of Cu atoms in Cu single crystal along the [010] and [111] directions, respectively. It is known that the space between two Cu atoms in Cu_6Sn_5 is 0.25478 nm along the [$\bar{2}$01] direction. Furthermore, the Cu atom space is 0.25560 nm along the [110] or [$\bar{1}$10] directions on the (001) plane, which is the same as that along the [1$\bar{2}$1], [$\bar{2}$11] or [11$\bar{2}$] directions on the (111) plane of Cu, as illustrated in Fig. 13b and c. Therefore, based on the difference in the atom spaces above, the misfit (α) of Cu atoms between the [$\bar{2}$01] direction of Cu_6Sn_5 and the [110], [$\bar{1}$10], [1$\bar{2}$1], [$\bar{2}$11] and [11$\bar{2}$] directions of Cu can be calculated as

$$\alpha = (0.25560 - 0.25478)/0.25478 = 0.32\%. \quad (2)$$

Based on the above analysis, it is obvious that the misfit of Cu atoms between Cu and Cu_6Sn_5 is extremely low (only 0.32%). The result is different from Suh and Tu's result [12] because the high-temperature η'-Cu_6Sn_5 phase structure was selected for analysis of Cu_6Sn_5 in Ref. [12]. It is well known that the interfacial energy will reduce with decreasing the misfit between the IMC and substrate [12]. If there is a low misfit direction on the substrate, Cu_6Sn_5 would preferentially nucleate along these low-misfit directions after the liquid-state reaction in order to minimize the interfacial energy, leading to the formation of the strong texture in Cu_6Sn_5 grains. According to the crystallographic relations illustrated in Fig. 13b and c, the Cu_6Sn_5 grains formed on (001) Cu single crystal should be preferentially elongated along the [110] and [$\bar{1}$10] directions, which is the same as the results in Ref. [12]. Since the [110] and [$\bar{1}$10] directions in Cu_6Sn_5 are perpendicular to each other, it is not difficult to understand why the Cu_6Sn_5 grains formed on (001) Cu single crystal were elongated along two perpendicular directions, as shown in Fig. 2b. However, the elongated directions of Cu_6Sn_5 grains formed on (111) Cu single crystal should become [1$\bar{2}$1], [$\bar{2}$11] and [11$\bar{2}$]. It should be pointed out that the angle between each pair of [1$\bar{2}$1], [$\bar{2}$11] and [11$\bar{2}$] directions in Cu_6Sn_5 is equal to 60° as illustrated in Fig. 13c. This is consistent with our experimental observations that the angle between all pairs of elongated directions of Cu_6Sn_5 grains formed on (111) Cu single crystal is about 60°, as shown in Fig. 4b, which has never been observed before. Fig. 13d and e are schematic diagrams of (010) Cu_6Sn_5 grains formed on (001) and (111) Cu single crystals. It can be seen that all the elongated directions of Cu_6Sn_5 grains formed on (111) Cu single crystal are [$\bar{2}$01]. The angle between the [100] and [$\bar{2}$01] directions of Cu_6Sn_5 grains was calculated to be 22.4°, which is quite close to our exper-

iment results (19.3°, 16.9°, 18.7°). Therefore, some orientation relationships between Cu_6Sn_5 grains and Cu single crystals can be deduced. For the Cu_6Sn_5 grains on (0 0 1) and (1 1 1) Cu single crystals, one obtains

$[\bar{2}01]_{Cu_6Sn_5}||[\bar{1}10]_{(001)Cu}$ and $[\bar{2}01]_{Cu_6Sn_5}||[110]_{(001)Cu}$,
$[\bar{2}01]_{Cu_6Sn_5}||[1\bar{2}1]_{(111)Cu}$, $[\bar{2}01]_{Cu_6Sn_5}||[\bar{1}\bar{1}2]_{(111)Cu}$
and $[\bar{2}01]_{Cu_6Sn_5}||[\bar{2}11]_{(111)Cu}$.

In summary, the regular array and the minimum misfit of Cu atoms should lead to the great differences in the morphologies and orientation relationships of Cu_6Sn_5 grains formed on (0 0 1) and (1 1 1) Cu single crystals. Compared with the Cu_6Sn_5 formed on polycrystalline Cu, regular Cu_6Sn_5 grains form more easily on (0 0 1) and (1 1 1) Cu single crystals because the minimum misfit of Cu atoms with Cu_6Sn_5 and Cu can be more easily achieved in the two crystals, and the minimum misfit of Cu atoms will decrease the nucleation driving force of strongly textured Cu_6Sn_5. Therefore, it can be concluded that the nucleation of Cu_6Sn_5 grains formed on (0 0 1) and (1 1 1) Cu single crystals is quite different from that on polycrystalline Cu [11,14,15]. The current experimental results provide new evidence that the orientations of Cu single crystals greatly influence the morphology of Cu_6Sn_5 grains.

4.2. Growth kinetic of Cu_6Sn_5 grains with different morphologies

During the liquid interfacial reaction, whether the morphology of the Cu_6Sn_5 grain is scallop-type or regular prism-type, the size of Cu_6Sn_5 grains will increase with increasing reflow time, as shown in Figs. 2–5. Fig. 14 shows the dependence of the size of Cu_6Sn_5 grains on the reflow time between Sn and Cu single crystals. This dependence follows: $r = C_1 t^k$, where r is the grain size, C_1 and k are constant, and t is the reflow time. From these results in Fig. 14, the constant k was calculated to be 0.31 and 0.30 for the scallop-type Cu_6Sn_5 grains formed on (0 1 1) and (1 2 3) Cu single crystals, respectively. These results are consistent with Kim and Tu's findings [11]. The constant k was calculated to be 0.19 and 0.24 for regular prism-type Cu_6Sn_5 grains formed on (0 0 1) and (1 1 1) Cu single crystals, respectively. This indicates that the growth mechanisms of Cu_6Sn_5 grains were also controlled by their morphology.

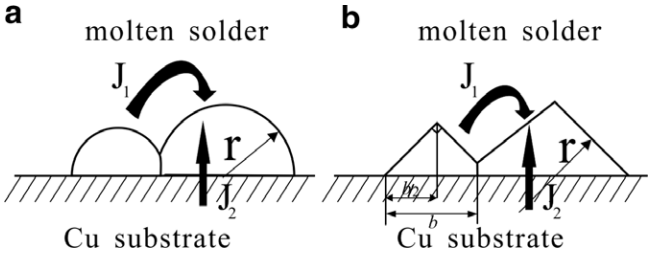

Fig. 15. Schematic diagram of the Cu flux for IMC grains with different morphologies: (a) scallop-type and (b) prism-type.

Fig. 15 is a schematic diagram of the Cu flux among the Cu_6Sn_5 grains with different morphologies. According to the Gibbs–Thomson effect and the analysis of Kim and Tu [11], the flux will be obtained as follows (the detailed derivation can be seen in Ref. [11]):

$$C_r = C_0 \exp\left(\frac{2\gamma\Omega}{rRT}\right), \tag{3}$$

$$J_1 = \frac{2\gamma\Omega D C_0}{3\delta RT}\frac{1}{\bar{r}}, \tag{4}$$

$$J_2 = \frac{\rho N_A A v(t)}{2\pi m N_p(t)}\frac{1}{\bar{r}^2}, \tag{5}$$

where C_r is the concentration of Cu in the molten at the surface of the grain, J_1 is the ripening flux, J_2 is the interfacial reaction flux, γ is the interfacial energy per unit area between Cu_6Sn_5 and molten Sn, r is the radius of the Cu_6Sn_5 grains; Ω is the molar volume of Cu_6Sn_5, R is a gas constant; T is the absolute temperature, N_A is Avogadro's constant, D is the diffusion coefficient of Cu in the liquid Sn, $v(t)$ is the consumption rate of Cu foil, $N_p(t)$ is the

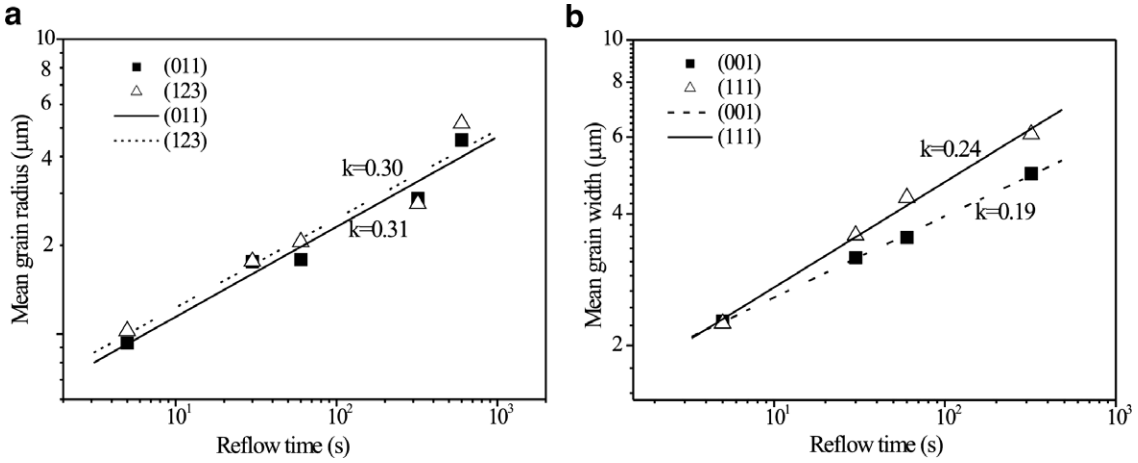

Fig. 14. Mean grain size of Cu_6Sn_5 vs. reflow times at 260 °C of Sn/Cu single crystals.

total number of Cu_6Sn_5 grains at the interface, ρ is the density of Cu, A is the total area of solder/Cu interface, m is the atomic mass of Cu, δ is the average grain separation distance, $\bar{r}$ is the mean grain size, and C_0 is the equilibrium concentration of Cu in Sn. From Eqs. (3)–(5), the growth equation for scallop-type Cu_6Sn_5 grains is (the detailed derivation can be seen in Ref. [11])

$$r^3 = \int \left(\frac{\gamma \Omega^2 D C_0}{3 N_A L R T} + \frac{\rho A \Omega v(t)}{4\pi m N_p(t)} \right) dt. \quad (6)$$

However, for the prism-type Cu_6Sn_5 grains, $r = \infty$, as illustrated in Fig. 15b, according to Eq. (3), one can get

$$C_r = C_0, \quad (7)$$

Therefore

$$J_1 = 0. \quad (8)$$

For a hemispherical Cu_6Sn_5 grain, the surface area is $2\pi\bar{r}^2$, but for the prism-type Cu_6Sn_5 grain, the surface area is $\sqrt{2}x\bar{b}^2$, as illustrated in Fig. 15b. Hence, we can also get

$$J_2 = \frac{\rho N_A A v(t)}{\sqrt{2} x m N_p(t)} \frac{1}{\bar{b}^2}, \quad (9)$$

where $x = l/b$, and l and b are the length and width of the prism-type Cu_6Sn_5 grains. This analysis indicates that the growth of prism-type Cu_6Sn_5 grains was only affected by the interfacial reaction flux (J_2). Then the mean width b of the prism-type Cu_6Sn_5 grains is

$$b^3 = \int \frac{2\rho A \Omega v(t)}{9 x m N_p(t)} dt = \frac{2\rho A \Omega}{9 x m} \int \frac{v(t)}{N_p(t)} dt. \quad (10)$$

Wang and Liu [22] found that the $v(t)$ can be expressed as $v(t) = 1.5 \times 10^{-5} t^{-0.76}$ for Sn/Cu at 250 °C ($T = 260$ °C in our experiment). Fig. 16 shows the number of Cu_6Sn_5 grains per square centimeter on different Cu single crystals, based on the relationship $N_p(t) = Ct^n$. For (0 1 1) and (1 2 3) Cu single crystals reflowed at 260 °C, $n = -0.611$, -0.602 (scallop-type Cu_6Sn_5), respectively. Substituting the two variable functions $v(t)$ and $N_p(t)$ into Eq. (6), one obtains $r \sim t^{1/3}$. This is consistent with our experimental results: $r \sim t^{0.31}$ and $r \sim t^{0.30}$ for (0 1 1) and (1 2 3) Cu single crystals, respectively. However, for (0 0 1) and (1 1 1) Cu single crystals reflowed at 260 °C, $n = -0.407$, -0.463 (prism-type Cu_6Sn_5), respectively. Substituting the two variable functions $v(t)$ and $N_p(t)$ into Eq. (10) yields $b \sim t^{0.21}$ and $b \sim t^{0.23}$ for (0 0 1) and (1 1 1) Cu single crystals, respectively, which are quite close to our experimental results: $b \sim t^{0.19}$ for (0 0 1) Cu single crystal, and $b \sim t^{0.24}$ for (1 1 1) single crystal. The above results indicate that the orientations of Cu single crystals also have much influence on the growth kinetics of Cu_6Sn_5 grains during the liquid-state interfacial reaction.

4.3. The morphologies of IMCs under liquid-state and solid-state conditions

As shown in Figs. 2d and 4d, the morphology of Cu_6Sn_5 grains changes from regular prism-type to scallop-type when the reflow time is increased to 600 s for the interfacial reaction between molten Sn (0 0 1) and (1 1 1) Cu single crystals. As is well known, the Cu_6Sn_5 grains were firstly formed during the interfacial reaction between Sn and Cu substrate, and then another IMC (Cu_3Sn) would form between the Cu_6Sn_5 layer and Cu substrate with increasing reflow time [3,15,18]. Therefore, on the (0 0 1) and (1 1 1) Cu single crystal surfaces, the regular prism-type Cu_6Sn_5 grains were firstly formed during the short reflow time (below 600 s). However, the Cu atoms coming from the Cu substrate would react with these regular prism-type Cu_6Sn_5 grains to form the Cu_3Sn layer at longer reflow times (above 600 s), as shown in Fig. 17. In this case, the nucleation of regular prism-type Cu_6Sn_5 grains would decrease with increasing reflow time, and the scallop-type Cu_6Sn_5 grains would begin to form. Therefore, the morphology of Cu_6Sn_5 grains was gradually transformed from regular prism-type into scallop-type.

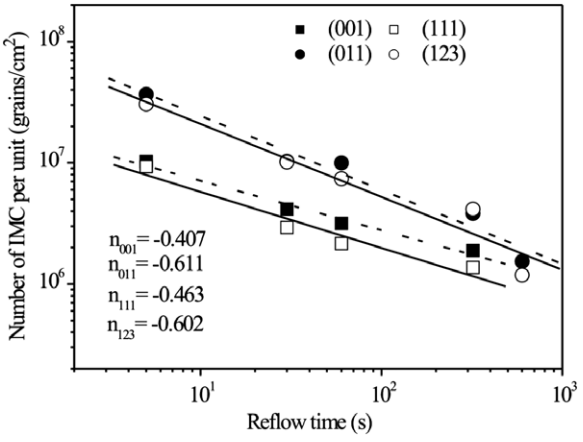

Fig. 16. Number of Cu_6Sn_5 grains per unit at the Sn/Cu single crystals vs. reflow times at 260 °C of Sn/Cu single crystals.

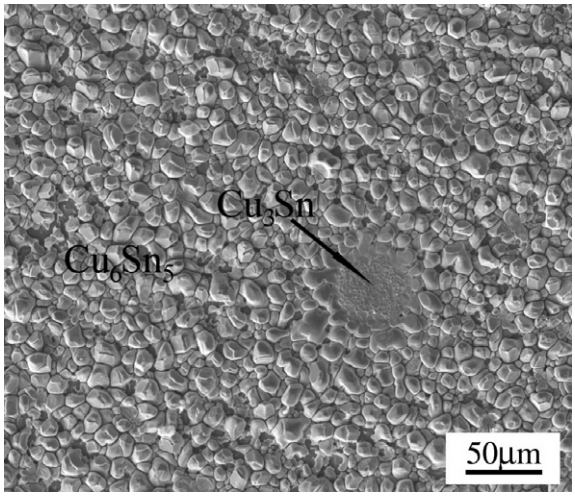

Fig. 17. Cu_3Sn grains formed on (0 0 1) Cu single crystal at reflow at 260 °C for 600 s.

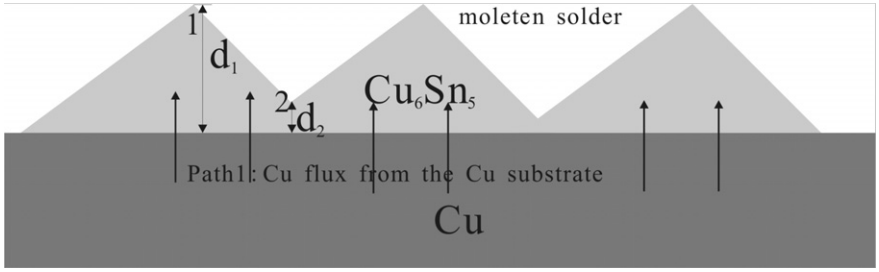

Fig. 18. Schematic diagram of Cu diffusion path during the solid-state aging.

Compared with the liquid-state interfacial reaction, the final morphology of Cu_6Sn_5 grains is also scallop-type for the solid-state interfacial reaction, as illustrated in Figs. 6–9. This can be attributed to the formation of the Cu_3Sn layer between the Cu substrate and the Cu_6Sn_5 layer. In addition, the morphology of the IMCs was found to change from prism-type to planar-type in our experiments with increasing aging time under the solid-state condition. However, it has been reported previously that the morphology of the IMCs changes from scallop-type to planar [11,15]. The same model was used to explain this phenomenon. Fig. 18 is a schematic diagram of the diffusion path of Cu during solid-state aging. It can be clearly seen that the growth of the prism-type Cu_6Sn_5 grains is only controlled by "path 1". According to Fig. 18, d_1 and d_2 are the distances between the Cu substrate and the two different points 1 and 2 of a prism-type Cu_6Sn_5 grain, respectively. It is obvious that $d_2 < d_1$, and the total diffusion coefficients of Sn and Cu through the Cu_6Sn_5 are the same; hence, it can be concluded that the growth velocity of Cu_6Sn_5 grains at point 2 should be higher than that at point 1. In this case, the prism-type Cu_6Sn_5 grains became planar with increasing aging time. As mentioned above, during the liquid/solid interfacial reaction, the ripening behavior of Cu_6Sn_5 grains formed on Cu single crystals is quite different from that on polycrystalline Cu [11,14,15]. Furthermore, the orientations of Cu single crystals also affect the ripening behaviors of the formed Cu_6Sn_5 grains.

5. Conclusions

Based on the experimental results and the above analysis, the following conclusions can be drawn.

On the (0 0 1) Cu single crystal surface, regular prism-type Cu_6Sn_5 grains align along two perpendicular preferential directions, whereas on the (1 1 1) Cu single crystal surface, the prism-type Cu_6Sn_5 grains are elongated along three preferential directions with an angle of 60° between each pair of directions. However, on (0 1 1) and (1 2 3) Cu single crystals, scallop-type Cu_6Sn_5 grains were widely detected except for few regular prism-type grains at localized regions. EBSD confirmed that there are some preferential orientations with low index between Cu_6Sn_5 grains and (0 0 1) or (1 1 1) Cu single crystal. In addition, the coarsening mechanisms of Cu_6Sn_5 grains with different morphologies are also affected by the orientations of Cu single crystals. When the reflow time is less than 600 s, regular prism-type Cu_6Sn_5 grains can be observed on the (0 0 1) and (1 1 1) Cu single crystal surfaces, but scallop-type Cu_6Sn_5 grains can be observed on all the Cu single crystal surfaces after prolonged aging for more than 600 s.

Experiments also revealed the evolution of the morphology of Cu_6Sn_5 grains formed between molten Sn and Cu single crystals under solid-state conditions. For (0 0 1) and (1 1 1) Cu single crystals, the morphologies of Cu_6Sn_5 grains first changed from prism-type to planar prism-type, and finally to scallop-type IMCs.

The growth kinetics of IMCs between Sn and Cu single crystals also displayed obvious dependence on the orientation of the Cu single crystals. The growth of the IMCs is still controlled by the diffusion mechanism. However, the diffusion coefficients, D, were calculated to be 1.96×10^{-17}, 2.96×10^{-17} and $2.96 \times 10^{-17}\,m^2\,s^{-1}$ for (0 1 1), (1 1 1) and (1 2 3) Cu single crystals, respectively.

Acknowledgments

The authors would like to thank W. Gao, P. Li, H.H. Su, X.H. Sang, G.L. Gong, J.T. Liu, J.T. Fan, F. Yang, P. Zhang and Q.S. Zhu for sample preparation, SEM observations, crystallographic analysis and stimulating discussion. This work was financially supported by the National Basic Research Program of China under Grant No. 2004CB619306, the "Hundred of Talents Project" by the Chinese Academy of Science and the National Outstanding Young Scientist Foundation under Grant No. 50625103.

References

[1] Abtew M, Selvaduray G. Mater Sci Eng R 2000;27:95.
[2] Zeng K, Tu KN. Mater Sci Eng R 2002;38:55.
[3] Lee TY, Choi WJ, Tu KN, Jang JW, Kuo SM, Lin JK, et al. J Mater Res 2002;17:291.
[4] Ren F, Nah JW, Tu KN, Xiong BS, Xu LH, Pang JHL. Appl Phys Lett 2006;89:141914.
[5] Kerr M, Chawla N. Acta Mater 2004;52:4527.
[6] Bae KS, Kim SJ. J Mater Res 2002;17:743.
[7] Wang FJ, Ma X, Qian YY. Scripta Mater 2005;53:699.
[8] He M, Chen Z, Qi GJ. Acta Mater 2004;52:2047.
[9] Wu BY, Zhong HW, Chan YC, Alam MO. J Mater Res 2006;21:2224.

[10] Fouassier O, Heintz JM, Chazelas J, Geffroy PM, Silvain JF. J Appl Phys 2006;100:043519.
[11] Kim HK, Tu KN. Phys Rev B 1996;53:16027.
[12] Suh JO, Tu KN, Tamura N. Appl Phys Lett 2007;91:051907.
[13] Prakash KH, Sritharan T. J Electron Mater 2002;31:1250.
[14] Wang HQ, Gao F, Ma X, Qian YY. Scripta Mater 2006;55:823.
[15] Lauril T, Vuorinen V, Kivilahti JK. Mater Sci Eng R 2005;49:1.
[16] Prakash KH, Sritharan T. Acta Mater 2001;49:2481.
[17] Li JF, Mannan SH, Clode MP, Whalley DC, Hutt DA. Acta Mater 2006;54:2907.
[18] Zhu QS, Zhang ZF, Shang JK, Wang ZG. Mater Sci Eng A 2006;435–436:588.
[19] Yang W, Messier RW, Felton LE. J Electron Mater 1994;23:765.
[20] Larsson AK, Stenberg L, Lidin S. Acta Crystallogr 1994;B50:636.
[21] Larsson AK, Stenberg L, Lidin S. Z Kristallogr 1995;210:832.
[22] Wang SJ, Liu CY. Acta Mater 2007;55:5401.